

Figure 9. Structures for $\text{Cu}(\text{L-His})_n$ complexes in aqueous solution at pH 7.3.

pattern and an even pattern for $^{214}\text{N}, ^{15}\text{N}$. Thus the resolution for the reverse Fourier transform is adequate to confirm that the odd pattern for $^{214}\text{N}, ^{15}\text{N}$ dominates the spectrum for cupric ion in the presence of excess histidine-1,3- $^{15}\text{N}_2$.

Discussion

Copper in the presence of excess histidine in frozen solutions is bound to four nitrogens from the imidazole ring of histidine, forming a nearly square-planar complex (Figure 9c).⁸ The present studies establish that a mixture of a histamine-like and glycine-like structures (Figure 9a,b) exists in the liquid phase. Our original purpose for the addition of excess histidine was to prevent aggregation of the sample upon freezing without affecting axial coordination from substances like perchlorate, dimethyl sulfoxide, or glycerol, which also prevent aggregation. It appears that excess histidine may prevent aggregation by occupying the weak, axial positions. Upon freezing, two of the donor atoms that form the square plane are altered whereby two imidazole nitrogens, which may have been axial ligands, replace amine nitrogens and/or carboxyl oxygens. The histamine-like structure, $\text{Cu}(\text{His})_2$, is the dominant species in the liquid phase (Figure 9b).

Often, nitrogen donor atoms from the imidazole moieties of histidine amino acid residues in proteins are bound to cupric ion. One question that is of primary interest to us is whether freezing

the sample promotes substitution of nitrogen donor atoms from imidazole for nitrogen from amine, peptide linkages, or carboxyl groups. If nitrogen from imidazole favorably competes with other donor atoms as the temperature is lowered, structural information in the frozen state could be misleading.

It is reassuring that all simulations are consistent with a one to two stoichiometry for $\text{Cu}(\text{His})_2$ in the liquid phase. Goodman et al.¹⁰ found two complexes, one histamine-like for both ligands and the other histamine-like for one ligand and glycine-like for the second ligand, as do we. Future studies should focus on the pH and ligand concentration dependence.

The most convincing argument for four nitrogen donor atoms comes from the Fourier transform of the spectrum for $\text{Cu}-^{214}\text{N}, ^{15}\text{N}$ (Figure 6). The lines obtained from the experimental data are shifted to lower frequency if two ^{15}N donor atoms and two ^{14}N donor atoms comprise the square plane. The reverse Fourier transforms are complicated. The best information comes from the outer lines, which correspond to the "highest frequency" pattern, i.e. the pattern with the smallest superhyperfine couplings. This pattern resembles the pattern expected from ^{14}N and ^{15}N (Table I). For example a nine-line pattern is obtained from the reverse Fourier transform from the experimental spectrum, $\text{Cu}-^{14}\text{N}$ -exptl, and simulated spectrum, $\text{Cu}-4^{14}\text{N}$; a seven-line pattern is obtained from the simulation for $\text{Cu}-3^{14}\text{N}$; a seven-line pattern is obtained for the experimental data for $\text{Cu}-^{14}\text{N}, ^{15}\text{N}$ and for the simulated data for $\text{Cu}-2^{14}\text{N}, ^{15}\text{N}$; and an eight-line pattern is obtained for the simulated data for $\text{Cu}-2^{14}\text{N}, ^{15}\text{N}$. Because the copper hyperfine lines are suppressed in the reverse Fourier transform, the number of lines in the reverse Fourier transform is one-fourth the number of lines in the simulated spectra. The simplified pattern is much easier to analyze than the original spectrum. The outermost peak in the spectrum for the Fourier transform domain and the pattern of its reverse Fourier transform are therefore diagnostic for the nitrogen hyperfine pattern (Table I). It is anticipated that the Fourier transform and reverse Fourier transform will be useful displays to unravel hyperfine coupling constants for spectra that are well resolved but complicated due to overlap of many lines. We plan to test these methods on the g_{\perp} region of immobilized copper square-planar complexes for which the magnitudes of the hyperfine couplings for copper and nitrogen are both about 15 G.

Registry No. N_2 , 7727-37-9; $\text{Cu}(\text{His})_2$, 16884-54-1.

Contribution from the Department of Chemistry,
Seoul National University, Seoul 151, Republic of Korea

Kinetics and Mechanism of the Metal Ion Catalyzed Hydrolysis of Acetylpyridine Ketoxime Pyridinecarboxylates

Junghun Suh,* Byung Nam Kwon, Woo Young Lee, and Sae Hee Chang

Received July 30, 1986

The kinetics of the $\text{Cu}(\text{II})$ - or $\text{Zn}(\text{II})$ -catalyzed hydrolysis of 2- and 3-acetylpyridine ketoxime esters of picolinic acid or nicotinic acid were studied. Analysis of the kinetic data revealed that the picolinyl pyridine of 2-acetylpyridine ketoxime picolinate (**2a**) does not act as a general-base catalyst but exerts only electronic effects. Thus, the metal ions bind at the oxime moiety in the hydrolysis of **2a** as well as 2-acetylpyridine ketoxime nicotinate and the metal-bound nucleophiles attack the ester linkage. On the other hand, the metal ions catalyze the hydrolysis of picolinyl esters containing 3-acetylpyridine ketoxime or *p*-nitrophenol leaving groups by binding at the ester carbonyl oxygen through chelation at the picolinyl moiety. The kinetic data obtained in this study indicate that these two mechanisms are comparably efficient in terms of the reactivity of the metal-substrate complexes.

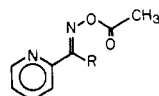
Metal ions catalyze some organic reactions by participating as Lewis acids. Elucidation of the catalytic roles of metal ions in these reactions provides important information on both inorganic and organic reactions.¹⁻³ In addition, possible catalytic roles of

metal ions in the action of metalloenzymes can be disclosed by the mechanistic studies of small model compounds.

Previously, we performed several kinetic studies on the $\text{Cu}(\text{II})$ - or $\text{Zn}(\text{II})$ -catalyzed hydrolysis of oxime esters **1a,b**.⁴⁻⁶ The

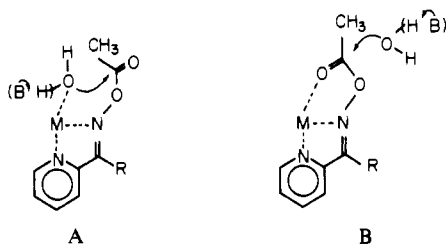
(1) Satchell, D. P. N.; Satchell, R. S. *Annu. Rep. Prog. Chem., Sect. A: Inorg. Chem.* **1979**, *75*, 25 and references therein.
(2) Dunn, M. F. *Struct. Bonding (Berlin)* **1975**, *23*, 61.

(3) Hipp, C. J.; Busch, D. H. *Coordination Chemistry*; Martell, A. E., Ed.; ACS Monograph 174; American Chemical Society: Washington, DC, 1978; Vol. 2, Chapter 2.



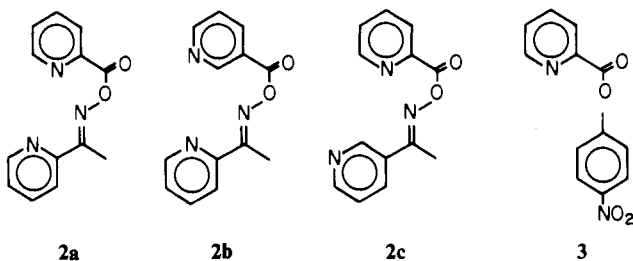
1a: R = H
b: R = CH₃

mechanism of these reactions is shown by A, as disclosed by the previous studies. The catalytic factors included in A are the increase in the leaving ability of the oximate anion and the intramolecular attack of the metal-bound nucleophiles at the ester linkage.



In the metal ion catalyzed hydrolysis of several other esters, coordination of carbonyl oxygen to a metal ion and the subsequent attack of hydroxide ion or water molecule at the polarized carbonyl group has been reported.¹ For the oxime esters, this corresponds to B. That the Zn(II)- or Cu(II)-catalyzed hydrolysis of **1a,b** does not proceed through B is presumably because the simultaneous coordination of the carbonyl oxygen and the two nitrogen atoms to the metal ion involves significant strain.

Our previous studies examined oxime esters derived from acetic acid. In the present investigation, the study has been extended to the hydrolysis of oxime esters derived from pyridinecarboxylic acids: 2-acetylpyridine ketoxime picolinate (**2a**), 2-acetylpyridine ketoxime nicotinate (**2b**), and 3-acetylpyridine ketoxime picolinate (**2c**). In addition, *p*-nitrophenyl picolinate (**3**) has been inves-



igated. Additional catalytic features are expected to arise when the pyridinecarboxyl groups are introduced. In this article, the mechanisms of the Cu(II)- or Zn(II)-catalyzed hydrolysis of **2a-c** and **3** are elucidated in relation to A and B.

Experimental Section

Materials. Oxime esters **2a-c** were prepared by the dropwise addition of an acetone solution (10 mL) of the corresponding oxime (0.7 g) to another acetone solution (15 mL) that contained both *N,N*-dicyclohexylcarbodiimide (1.2 g) and the corresponding pyridinecarboxylic acid (0.6 g) over a period of 1 h at 0 °C. The resulting mixture was further stirred for 4 days at room temperature. Then, *N,N*-dicyclohexylurea was removed by filtration and the solvent was removed under reduced pressure. The solid materials obtained were separated on silica gel either by column chromatography or by thin-layer chromatography. The products were further purified by recrystallization from acetone-hexane: mp 120–123 °C for **2a**, 125–128 °C for **2b**, and 154–157 °C for **2c**. Ester **3** was prepared according to the reported procedures;⁷ mp 144–147 °C (lit.⁷ mp 144–146 °C).

Zinc chloride and cupric chloride were obtained by dissolving the corresponding oxides (Aldrich, "Gold Label") with hydrochloric acid. The solutions were evaporated, and the wet chlorides were dried under an infrared lamp. Water was distilled and deionized prior to use in kinetic studies.

(4) Suh, J.; Lee, E.; Jang, E. S. *Inorg. Chem.* **1981**, *20*, 1932.

(5) Suh, J.; Cheong, M.; Suh, M. P. *J. Am. Chem. Soc.* **1982**, *104*, 1654.

(6) Suh, J.; Han, H. *Bioorg. Chem.* **1984**, *12*, 177.

(7) Sigman, D. S.; Jorgensen, C. T. *J. Am. Chem. Soc.* **1972**, *94*, 1724.

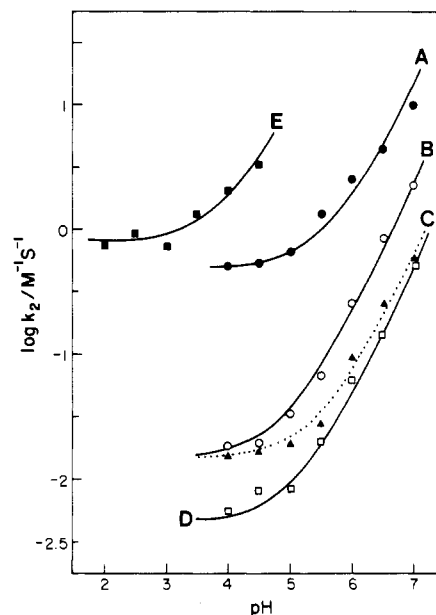


Figure 1. pH dependence of k_2 for the Zn(II)-catalyzed hydrolysis of **2a** (A), **2b** (B), **2c** (C), and **3** (D) and for the Cu(II)-catalyzed hydrolysis of **3** (E).

Table I. Parameter Values for the Zn(II)-Catalyzed Hydrolysis of the Oxime Esters

compd	k_w , M ⁻¹ s ⁻¹	k_{OH} , M ⁻² s ⁻¹
2a	0.50	1.4×10^8
2b	0.015	2.4×10^7
2c	0.015	6.3×10^6
3	0.0042	5.2×10^6
1a ^a		1.7×10^6
1b ^b	0.045	1.5×10^7

^a Reference 4. ^b Reference 6.

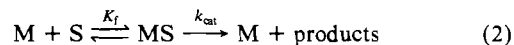
Kinetic Measurements. Reaction rates were measured with a Beckman 5260 UV/vis spectrophotometer. The temperature was controlled to within ± 0.1 °C with a Lauda Brinkmann Model RC3 circulator. pH measurements were performed with a Fisher Accumet Model 525 pH meter. The ionic strength was adjusted with sodium chloride to either 0.3 in Cu(II)-catalyzed reactions or 1.0 in Zn(II)-catalyzed reactions. Buffers (0.02 M) used were chloroacetic acid (pH 2.5–3), acetic acid (pH 3.5–5), and 2-morpholinoethanesulfonic acid (pH 5.5–7). Stock solutions of the substrates were prepared in acetonitrile, and the reaction mixtures contained 0.8% (v/v) acetonitrile. Reaction rates were measured with initially added 1×10^{-4} M substrate. Spectra of the product solutions obtained after the metal ion catalyzed hydrolysis of the ester substrates agreed with those obtained by mixing the expected hydrolysis products under identical conditions.

Results

In the Zn(II)-catalyzed hydrolysis of **2a-c** and **3**, the pseudo-first-order rate constant (k_0) was proportional to [Zn(II)], and the proportionality constant (k_2) was measured at several pHs. The pH dependence of k_2 for the Zn(II)-catalyzed hydrolysis of **2a-c** and **3** is illustrated in Figure 1. The pH profiles of k_2 were analyzed further according to eq 1, and the values of k_w and k_{OH} calculated therefrom are summarized in Table I.

$$k_2 = k_0/[M] = k_w + k_{OH}[\text{OH}^-] \quad (1)$$

In the Cu(II)-catalyzed hydrolysis of **2b** and **2c**, saturation behavior was manifested by k_0 with respect to [Cu(II)]. The same saturation kinetic behavior has been observed in the Cu(II)-catalyzed hydrolysis of **1a**,⁵ which was analyzed according to the scheme of eq 2. The rate expression derived from this scheme



$$k_0 = k_{cat}[M]/(1/K_f + [M]) \quad (3)$$

$$1/k_0 = 1/k_{cat} + (1/k_{cat}K_f)(1/[M]) \quad (4)$$

Table II. Parameter Values for the Cu(II)-Catalyzed Hydrolysis of the Oxime Esters

compd	condition	parameter values
2a		$k_{\text{cat}}^w > 0.7 \text{ s}^{-1}$ ^c
2b	pH 2.0	$k_{\text{cat}} = 0.057 \pm 0.003 \text{ s}^{-1}$ $K_f = 400 \pm 30 \text{ M}^{-1}$
	pH 3.0	$k_{\text{cat}} = 0.20 \pm 0.01 \text{ s}^{-1}$ $K_f = 330 \pm 30 \text{ M}^{-1}$
2c	pH 2.0	$k_{\text{cat}} = 0.16 \pm 0.01 \text{ s}^{-1}$ $K_f = 27 \pm 3 \text{ M}^{-1}$
	pH 3.0	$k_{\text{cat}} = 0.14 \pm 0.01 \text{ s}^{-1}$ $K_f = 22 \pm 2 \text{ M}^{-1}$
3	water path	$k_w = 0.80 \text{ M}^{-1} \text{ s}^{-1}$
	hydroxide path	$k_{\text{OH}} = 1.0 \times 10^{10} \text{ M}^{-2} \text{ s}^{-1}$
1a ^a	water path	$k_{\text{cat}}^w = 0.017 \text{ s}^{-1}$ $K_f = 75 \text{ M}^{-1}$
	hydroxide path	$k_{\text{cat}}^{\text{OH}} = 3.0 \times 10^8 \text{ M}^{-1} \text{ s}^{-1}$ $K_f = 75 \text{ M}^{-1}$
1b ^b		$k_{\text{cat}}^w > 0.7 \text{ s}^{-1}$ ^c

^a Reference 5. ^b Reference 6. ^c The reaction was complete within the manual mixing period, and correct measurement of the parameter values was not possible.

is eq 3, which is transformed into eq 4. From the linear plot of $1/k_0$ against $1/[\text{Cu(II)}]$ (eq 4), the values of k_{cat} and K_f are obtained for the Cu(II)-catalyzed hydrolysis of **2b** and **2c**, which are summarized in Table II. Kinetic data for the Cu(II)-catalyzed hydrolysis of **2b** and **2c** were not obtained at pHs higher than those indicated in Table II because of very fast rates.

For the Cu(II)-catalyzed hydrolysis of **2a**, the reaction was complete within the manual mixing period (ca. 5 s) at 2 mM [Cu(II)] and pH 2–3. Thus, accurate kinetic measurement was not carried out. Although k_{cat} and K_f were not correctly estimated, the half-life of the Cu(II) complex of **2a** is less than 1 s and, thus, the corresponding k_{cat} is greater than 0.7 s^{-1} (Table II). In the Cu(II)-catalyzed hydrolysis of **1b**, the kinetic parameters have not been estimated also due to fast rates as indicated in Table II.⁶

In the Cu(II)-catalyzed hydrolysis of **3**, k_0 was proportional to [Cu(II)]. The proportionality constant k_2 was measured at several pHs, and its pH dependence is illustrated in Figure 1. The pH profile was further analyzed according to eq 1, and the values of k_w and k_{OH} obtained therefrom are summarized in Table II.

Rates of the spontaneous hydrolysis of **2a–c** and **3** were negligible compared with those of the metal-catalyzed reactions at identical pHs.

Discussion

Depending on the nature of the substrate and the metal ion, k_0 is proportional to [M] or manifests saturation behavior with respect to [M]. Both of these have been observed with the Cu(II)- or Zn(II)-catalyzed hydrolysis of **1a** and **1b** and have been explained in terms of complex formation between metal ion and the substrate prior to ester hydrolysis (eq 2).^{4–6} Thus, the saturation kinetic behavior is observed when $1/K_f$ is comparable to [M] (eq 3), while k_0 is proportional to [M] with the proportionality constant being $k_{\text{cat}}K_f$ when K_f is much smaller than $1/[\text{M}]$.

When the functional groups of the substrate do not ionize over the pH range investigated,⁸ K_f is independent of pH. On the other hand, the process of k_{cat} involves both the water path and the hydroxide path (eq 5).⁵ Then, k_w and k_{OH} of eq 1 represent $k_{\text{cat}}^w K_f$ and $k_{\text{cat}}^{\text{OH}} K_f$, respectively.

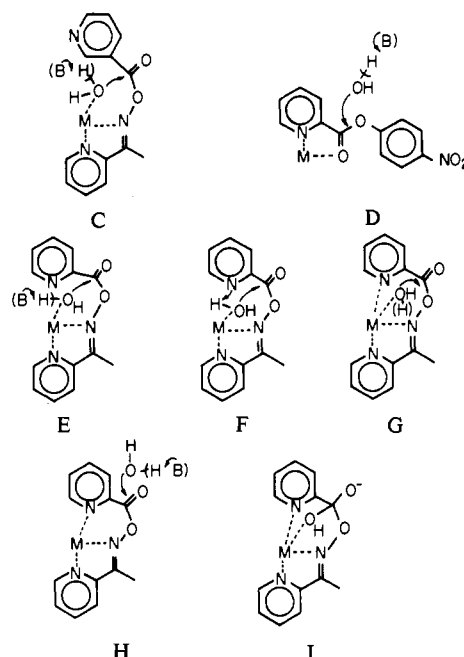
$$k_{\text{cat}} = k_{\text{cat}}^w + k_{\text{cat}}^{\text{OH}}[\text{OH}^-] \quad (5)$$

Among the four ester substrates investigated in the present study, the mechanism of the metal-catalyzed hydrolysis of **2b** is

(8) The pyridine nitrogen atoms of the pyridyl oxime moieties⁵ and the pyridinecarboxyl portions⁹ of **2a–c** or **3** do not significantly ionize over the pH range investigated in this study.

(9) Jencks, W. P.; Regenstein, J. *Handbook of Biochemistry and Molecular Biology*, 3rd ed.; Fasman, G. D., Ed.; CRC: Cleveland, OH, 1976; Vol. I, p 305.

most obvious because the nicotinylnitrogen is geometrically suited neither for metal chelation nor for participation as a general base. Thus, a mechanism (C) identical with A can be assigned to **2b**.¹⁰



In addition, the only chelation site available in **3** is the picolinyl portion and the metal ion catalyzed hydrolysis of **3** would involve the complexation mode indicated by D.

Several mechanisms (E–H) are possible for the metal ion catalyzed hydrolysis of **2a**, as the picolinyl nitrogen atom can act either as a general base or as an additional coordination site.

Compared with C, E includes only different electronic effects of the picolinyl ring while F and G assume additional catalytic factors and H assumes a quite different reaction path. If substantial rate increases are observed for **2a** in comparison with the case for **2b** and the rate increases cannot be accounted for by the different inductive effects exerted by picolinyl and nicotinylnitrogen, additional catalytic factors or new mechanisms are needed to explain the kinetic results. Conversely, if the rate difference can be attributed to the different electronic effects alone, it is very likely that the two substrates involve the same mechanism.

Among E–H, G can be excluded most readily in view of the ring strain involved in the tetrahedral intermediate (I) and, consequently, in the transition state.¹¹ Examination of molecular models indicates that the polycyclic ring system formed around the central metal ion in I should be highly strained when the configuration of the central metal atom is either planar or tetrahedral.

In pyridine derivatives, electron density at the 2-position is lower than that at the 3-position.¹³ Thus, the picolinyl group is more electron withdrawing than the nicotinylnitrogen. Between C and E, k_{cat} should be more favorable for E as the electrophilicity of the carbonyl carbon is greater in E. This is verified by the kinetic data measured with the Cu(II)-catalyzed hydrolysis of **2a** and **2b**. On the other hand, K_f should be more favorable for C as the

(10) The values of kinetic parameters measured for **2b** are not much different from those for **1a** and **1b** (Tables I and II). Considering the differences in the inductive and steric effects of the nicotinylnitrogen and the acetyl groups as well as the conjugation of the ester bond with the pyridine ring in **2b**, the rate data are consistent with the identical mechanisms for these esters.

(11) Nucleophilic reactions on acyl derivatives proceed through the formation of tetrahedral intermediates like I.¹² Since the tetrahedral intermediates are much more unstable than the reactants or the products, transition states should resemble tetrahedral intermediates in accordance with Hammond's postulate (Hammond, G. S. *J. Am. Chem. Soc.* **1955**, *77*, 334).

(12) Gresser, M. J.; Jencks, W. P. *J. Am. Chem. Soc.* **1977**, *99*, 6963.

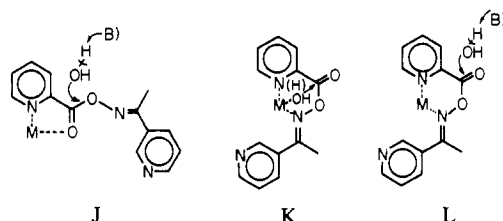
(13) Smith, D. M. *Comprehensive Organic Chemistry*; Barton, D., Ollis, W. D., Eds.; Pergamon: Oxford, England, 1979; Vol. 4, p 14.

electron density of the oxime nitrogen is greater in **2c**. The k_{OH} ($=k_{\text{cat}}^{\text{OH}}K_f$) value for the Zn(II)-catalyzed hydrolysis of **2a** is greater than that of **2b**. This is compatible with C and E. The inductive effects of the picolinyl and nicotinyl rings should be exerted to a much lesser extent on the oxime nitrogen than on the carbonyl carbon as the latter is located closer to the pyridine ring. Therefore, the inductive effect should be primarily reflected on k_{cat} , and $k_{\text{cat}}K_f$ should be greater for **2a** than for **2b**.

In the Zn(II)-catalyzed hydrolysis of **2a** and **2b**, k_w is 33-fold greater for **2a** while k_{OH} is only 6-fold greater for **2a**. This is also consistent with C and E. As discussed above, k_w and k_{OH} represent $k_{\text{cat}}^wK_f$ and $k_{\text{cat}}^{\text{OH}}K_f$, respectively. The ratio $k_w(\mathbf{2a})/k_w(\mathbf{2b})$, which is greater than the ratio $k_{\text{OH}}(\mathbf{2a})/k_{\text{OH}}(\mathbf{2b})$, therefore, reflects the greater selectivity manifested by k_{cat}^w compared with that of $k_{\text{cat}}^{\text{OH}}$ toward **2a** and **2b**. In C and E, k_{cat}^w and $k_{\text{cat}}^{\text{OH}}$ represent the intramolecular attack by the metal-bound water molecule and hydroxide ion, respectively. According to the reactivity-selectivity relationship, the less reactive attack by the metal-bound water molecule should exhibit greater selectivity. Therefore, the 5-fold greater selectivity manifested by the water path is consistent with C and E.¹⁴

The rate differences between **2a** and **2b** are explained by C and E, and it is not necessary to assume an additional catalytic factor (F) or a different mechanism (H) in order to explain the greater rates for **2a**. It is not likely, therefore, that the picolinyl ring of **2a** acts either as a general base in the water path or as an additional chelating ligand.

In the metal ion catalyzed hydrolysis of **2c**, the 3-acetylpyridine ketoxime moiety cannot form a chelate. Instead, chelates can be formed by using the picolinyl pyridine as in J-L. Only activation



of the carbonyl group is assumed in J, while an increase in the leaving ability of the oximate ion is also assumed in K or L.

Mechanism J is essentially identical with D. For D and J, K_f would be greater for **2c** and k_{cat} would be more favorable for **3** as *p*-nitrophenol ($\text{p}K_a = 7.1^9$) is more electron withdrawing than pyridine oximes ($\text{p}K_a = 10\text{--}11^{15}$).

In D and J, the rate-limiting step should be the formation, instead of breakdown, of the tetrahedral intermediate, as the leaving ability of hydroxide ion from the intermediate is much smaller than that of the *p*-nitrophenolate or 3-acetylpyridine

ketoximate ion.¹² When the formation of the tetrahedral intermediate is rate-limiting in the nucleophilic reactions on esters, $\beta_{\text{LG}} (= \Delta \log k / \Delta \text{p}K_{\text{LG}}; \text{p}K_{\text{LG}}$ is the $\text{p}K_a$ of the leaving group) is about 0.3.^{12,16} Thus, the difference in the basicities of the leaving groups would be reflected on k_{cat} to a small extent. The value of $k_{\text{cat}}^wK_f$ in the Cu(II)-catalyzed hydrolysis of **2c** is about 4 times greater than that of **3** (Table II). This is mainly due to the greater K_f for **2c**, which is consistent with the greater electron density on the carbonyl oxygen atom of **2c** compared with that of **3**. The 1.2-fold greater k_{OH} for the Zn(II)-catalyzed hydrolysis of **2c** compared with that for **3** is also attributable to the greater K_f for **2c** in spite of its smaller $k_{\text{cat}}^{\text{OH}}$. The ratio $k_w(\mathbf{2c})/k_w(\mathbf{3})$ is about 3 times greater than the ratio $k_{\text{OH}}(\mathbf{2c})/k_{\text{OH}}(\mathbf{3})$ in the Zn(II)-catalyzed reactions (Table I). This is also accounted for by the reactivity-selectivity relationship as was discussed above with the rate data for **2a** and **2b**. The rate data observed for **2c** and **3**, therefore, are explained by the same mechanism (D and J), and assumption of totally different mechanisms (D and K/L) is not necessary.

The structural differences between **2b** and **2c** result in different mechanisms for the respective metal ion catalyzed hydrolysis. The K_f values measured in the Cu(II)-catalyzed reactions are less favorable for **2c**, indicating that the picolinyl moiety of **2c** is less efficient than the 2-acetylpyridine ketoxime moiety of **2b** as a chelating ligand. This can be taken to indicate the greater basicity of the imine nitrogen compared with that of the carbonyl oxygen. Similar k_{cat} values were observed for the Cu(II)-catalyzed hydrolysis of **2b** and **2c** at pH 2 and 3. This indicates that the two mechanisms exemplified by C and J, i.e., the mechanism that includes the intramolecular nucleophilic attack by metal-bound nucleophiles at the ester as well as the increased leaving-group ability and the mechanism that involves the nucleophilic attack at the metal-bound carbonyl group by external nucleophiles, are comparably efficient in terms of k_{cat} . When both of these mechanisms are available (e.g., A and B), it is the formation constant (K_f) that decides the favorable reaction path. The formation constant in turn depends on the geometry and the Lewis basicity of the ligand atoms.

In the action of some metalloenzymes, the two mechanisms exemplified by A and B may represent possible catalytic roles of the active-site metal ions. In this case, the favorable mechanism could be largely decided by the stability of the respective metal complexes formed within the active sites of the enzyme-substrate complexes, as the results of the present study implicate.

Acknowledgment. This work was supported by the Basic Science Research Institute Program (1986), Ministry of Education, Republic of Korea, and the Korea Science and Engineering Foundation.

Supplementary Material Available: Listings of raw kinetic data for the Zn(II)-catalyzed hydrolysis of **2a**–**c** and **3** and for the Cu(II)-catalyzed hydrolysis of **2b,c** and **3** (6 pages). Ordering information is given on any current masthead page.

(14) The general-base catalysis involved in F is operative only in the water path. It is unreasonable to assume an additional catalytic factor like general-base catalysis in order to explain only 5-fold greater selectivity observed in the water path compared with that of the hydroxide path.
 (15) Suh, J.; Suh, M. P.; Lee, J. D. *Inorg. Chem.* **1985**, *24*, 3088.

(16) Suh, J.; Lee, B. H. *J. Org. Chem.* **1980**, *45*, 3103.